Pergamon

Tetrahedron 56 (2000) 9809–9818

TETRAHEDRON

Preferred Secondary Structures as a Possible Driving Force for Macrocyclization

Samuel Reyes, Mookda Pattarawarapan, Sudipta Roy and Kevin Burgess*

Department of Chemistry, Texas A & M University, P.O. Box 30012, College Station, TX 77842-3012, USA

Received 10 May 2000; accepted 2 August 2000

Abstract—The purpose of the work described in this paper was to explore links that may exist between conformational bias in macrocyclic products and the ease with which they are formed in solid phase S_NAr reactions. Solid phase synthesis of compounds **2** proceeds more efficiently than of compounds **3** under similar conditions. Compounds **2** were designed to mimic β-turn conformations in the dipeptide residues whereas compounds **3** were thought to be unable to show a similar conformational preference. The second assertion was shown to be correct but, surprisingly, CD, NMR, and molecular simulation experiments for **2a** indicate another conformation is preferred in solution. This may involve H-bonding of the asparagine side-chain to a backbone amide-carbonyl. Molecular dynamics simulations indicate that cyclization to form compound **2a** is statistically more favorable than that to form **3a**. © 2000 Elsevier Science Ltd. All rights reserved.

Introduction

Some previous studies from our group have focussed on development of solid phase syntheses of β-turn mimetics[1] that could be applied in high-throughput parallel syntheses.[2] It was proposed that some 14-membered ring macrocycles would be ideal targets for this purpose. Subsequently, it was shown that systems of the general type **1** could be formed efficiently on a solid phase, and that they could adopt type I turn conformations in solution.[3–5] These observations support the validity of a working hypothesis that was formulated at the inception of these studies. Specifically, it was reasoned that 14-membered ring systems could be designed wherein a non-peptide template held a dipeptide fragment into the desired conformation by forming two C^{10} conformations that share a C═O···H–N edge. These systems are therefore reminiscent of the well-known turn-extended-turn conformations of cyclic hexapeptides,[6,7] except that the ring size is smaller.

The critical synthetic step in the formation of compounds **1** is macrocyclization of linear precursors via an on-resin S_NAr reaction. This must be efficient for formation of materials **1**. However, the syntheses that have been performed so far do not elucidate the role of the dipeptide conformation in this macrocyclization process. It is not clear if formation of a β-turn conformation in the linear precursor increases the efficiency of the macrocyclization process.

The studies described here feature two similar macrocyclization processes to give the 14-membered ring systems **2** and **3**. Molecular modeling suggested that compounds **2** can form β-turn conformations, whereas the macrocycles **3** could not. Simple molecular models also suggested that even though the macrocycles **3** could not adopt β-turn conformations, they could cyclize to relatively unstrained rings. The short-term objectives of this study were therefore to: (i) compare the product yields and purities in solid phase syntheses of compound types **2** and **3**; (ii) use computer-aided molecular simulations, CD, and NMR experiments to elucidate preferred conformations of these products in

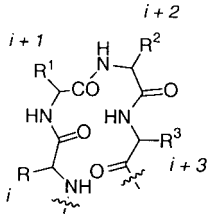

β-turn structure

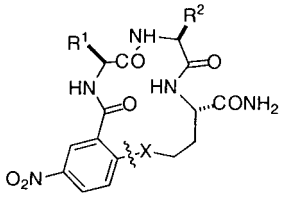

1
X = O or NH

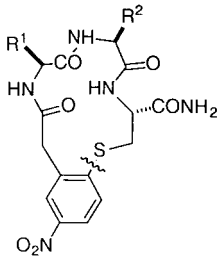

2

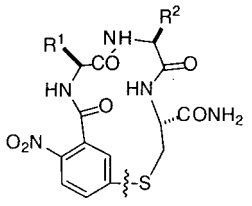

3

Keywords: S_NAr; macrocyclizations; β-turns; solid phase synthesis.

* Corresponding author. Tel.: +1-409-845-4345; fax: +1-409-845-8839; e-mail: burgess@tamu.edu

0040–4020/00/$ - see front matter © 2000 Elsevier Science Ltd. All rights reserved.
PII: S0040-4020(00)00888-7

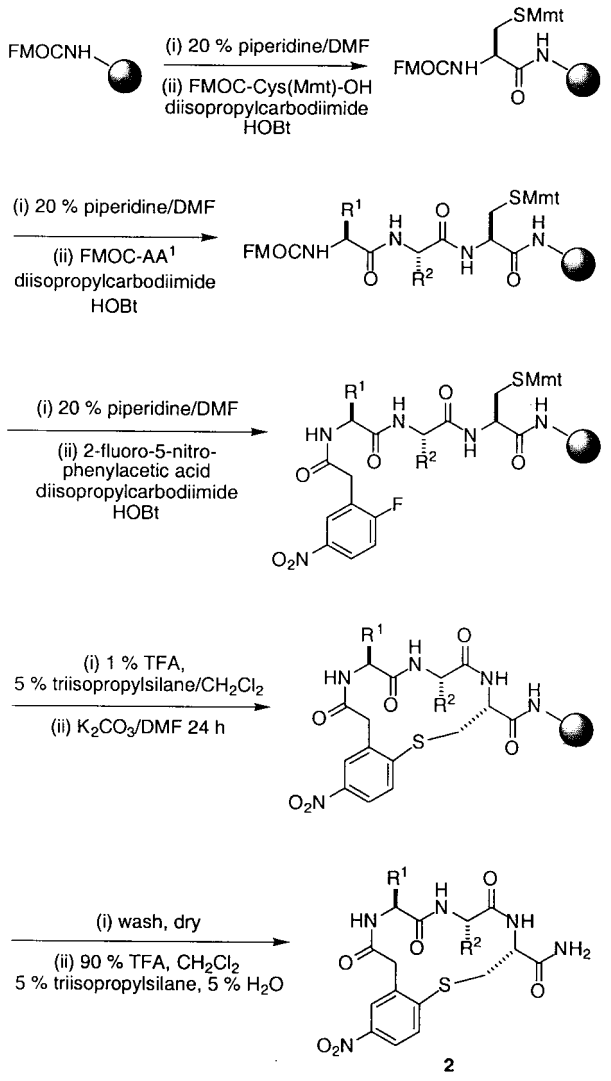

Scheme 1. Solid phase synthesis of compounds **1**.

solution; and, (iii) to use the data obtained in (i) and (ii) to infer indirect evidence for the role of β-turn conformations in the macrocyclization event.

The strategy outlined above cannot be a rigorous test for macrocyclizations driven by β-turn conformations; direct comparison of the activation energies for the on-resin macrocyclization steps would be required to do this, and that data is not conveniently accessible. However, two additional factors made these particular studies desirable for our long-term plans for the target compounds, i.e. to mimic or disrupt specific protein–protein interactions that feature β-turns. First, even though desirable conformational attributes of the peptidomimetics can be easily predicted and experimentally determined, other factors such as pharmacokinetics cannot. Consequently, compounds containing a variety of non-peptidic scaffolds will probably have to be screened to find a viable lead. Second, some loop regions found in proteins do not adopt ideal β-turn structures, hence it is possible that the mimics **3** will have unique and valuable characteristics for loop mimics. At the very least, structures **3** are potential controls to gauge the importance of β-turn conformations in various bioassays. In summary, our overall research program would be advanced if efficient solid phase syntheses of macrocycles **2** and/or **3** could be devised, and their preferred conformations determined.

Results and Discussion

Solid phase syntheses of compounds 2 and 3

Scheme 1 shows the synthetic route that was used to obtain compounds **2**. Briefly, monomethoxytrityl-protected (Mmt) cysteine, and two amino acids were added to a TentaGel resin functionalized with the Rink linker using standard peptide coupling conditions. 2-Fluoro-5-nitrophenylacetic acid was then used to cap the tripeptide. Removal of the monomethoxytrityl protecting group without cleaving the peptide from the resin was effected using dilute trifluoroacetic acid in the presence of tri-*iso*-propylsilane as a scavenger. On-resin macrocyclization was achieved by treating the peptide with potassium carbonate in DMF for 24 h, and then the peptide was cleaved from the resin using more concentrated TFA.

Table 1 shows the percent purities and yields of the products **2** obtained as shown in Scheme 1. The purities range from 76–92% and the isolated yields were between 37 and 59%. HPLC analyses of the crude reaction mixtures did not show any byproducts that prevailed above the others hence none were isolated. All the compounds were isolated via preparative HPLC, and characterized by MALDI-MS and proton NMR.

Syntheses of compounds **3** (Scheme 2) were achieved using a route very similar to that for compounds **2**, except that the capping group was 5-fluoro-2-nitrobenzoyl chloride. However, the proportions of compounds **3** in the crude materials were less than in the corresponding syntheses of **2**; they ranged from 36–72% (Table 2). This time there was

Table 1. Purity and yield data for compounds **2**

Compound[a]	R^1	R^2	Purity (%)	Isolated yield (%)
2a	CH_2CONH_2	$(CH_2)_4NH_2$	89	57
2b	$CH(CH_3)CH_2CH_3$[b]	$(CH_2)_4NH_2$	92	50
2c	$CH(CH_3)CH_2CH_3$[b]	$(CH_2)_3NHC(=NH)NH_2$	86	37
2d	$(CH_2)_3NHC(=NH)NH_2$	H	76	40
2e	$(CH_2)_4NH_2$	$CH(CH_3)(OH)$[c]	85	59

[a] All peptides were synthesized using TentaGel S RAM resin (0.26 mmol/g).
[b] Fmoc-Ile-OH used had the *S*-configuration of the side-chain.
[c] Fmoc-Thr(^{t}Bu)-OH used had the *R*-configuration of the side-chain.

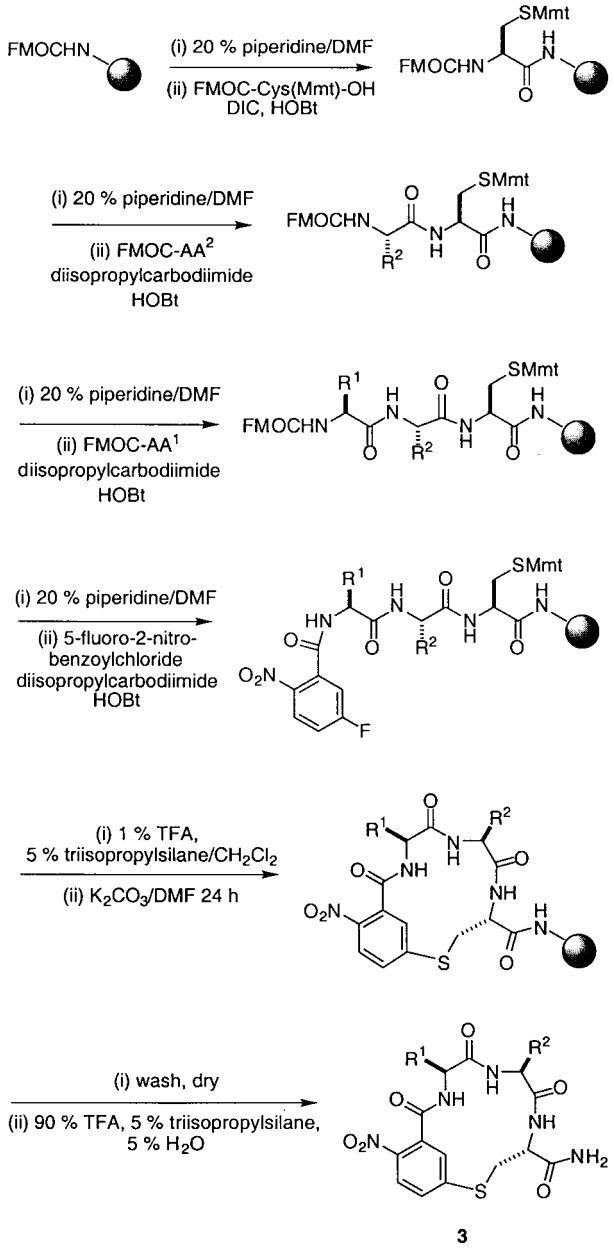

Scheme 2. Solid phase synthesis of compounds **2**.

an impurity type that was consistently observed and, on the basis of MALDI-MS, proton NMR, and our previous experience with similar macrocyclizations, the structure of these impurities can be assigned as the dimeric macrocyclization products **4**. These data indicate that macrocyclizations to form compounds **2** are more efficient than those to form compounds **3**.

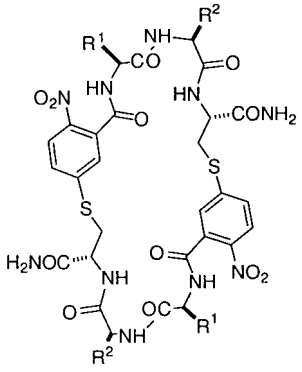

Conformational analyses of compounds 2a and 3a

Three techniques were used to deduce the conformational preferences of compounds **2a** and **3a**: (i) one- and two-dimensional NMR methods, (ii) CD spectroscopy; and, (iii) molecular simulations. The molecular simulations were performed without using any constraints from NMR, so good agreement with the predicted conformations and the observed physical data is a sign of the validity of the modeling approach.

Type I β-turns are thought to give CD spectra with minima just above 200 nm, while type II turns give maxima in the same region.[8] Fig. 1 shows the CD spectra of compounds **2a** and **3a**. Neither of these spectra fit well with the anticipated bandshapes for type I or type II turns; in both cases the ellipticity maxima/minima occur at longer wavelengths than would be anticipated for clearly defined turn structures.

Several NMR methods were used to deduce the preferred molecular conformations in this study. Temperature coefficients were measured for the N*H* chemical shifts in DMSO solution; a value of less than 3.0 ppb is indicative of a solvent shielded or H-bonded N*H*.[9–11] Rates of H/D exchange were recorded for the compounds in D_2O to give a second indication of solvent accessibility of the N*H* atoms but, in fact, the exchanges rates were too fast to measure for both compounds.[12] Coupling constants were determined for NH-to-C$^{\alpha}$*H* and fitted to an adjusted Karplus relationship to provide information about the relative orientations of these protons.[13] Finally, ROESY spectra[14] were

Table 2. Purity and yield data for compounds **3**

Compound[a] (**3** or **4**)	R^1	R^2	Purities (%)		Isolated yields (%)	
			3	**4**	**3**	**4**
a	CH_2CONH_2	$(CH_2)_4NH_2$	72	15	28	1
b	$CH(CH_3)CH_2CH_3$[b]	$(CH_2)_4NH_2$	67	25	17	4
c	$CH(CH_3)CH_2CH_3$[b]	$(CH_2)_3NHC(=NH)NH_2$	70	29	21	5
d	$CH(CH_3)(OH)$[c]	H	62	28	26	8
e	CH_2CO_2H	$CH(CH_3)CH_2CH_3$[b]	36	60	10	4

[a] All peptides were synthesized using Rink Amide MBHA resin (0.54 mmol/g).
[b] Fmoc-Ile-OH used has the *S*-configuration of the side-chain.
[c] Fmoc-Thr(^{t}Bu)-OH used has the *R*-configuration of the side-chain.

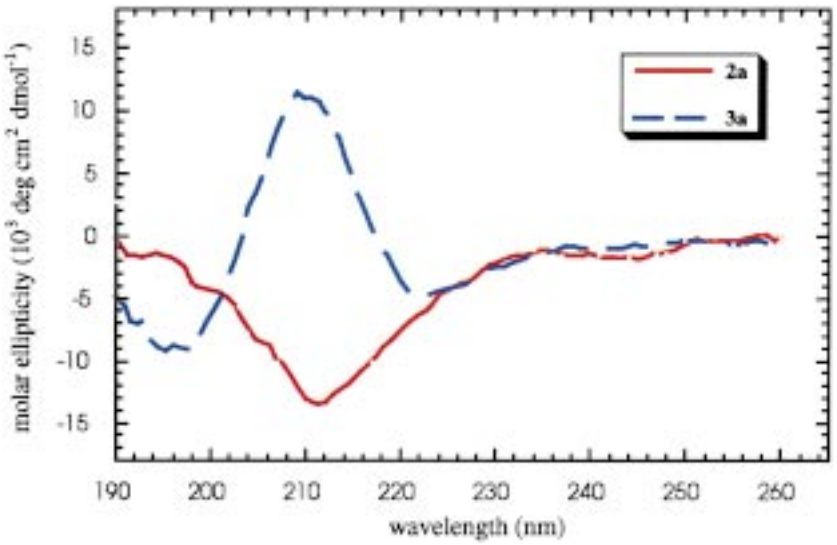

Figure 1. CD Spectra in 1:4 MeOH/H_2O.

recorded to give an indication of the proximity of various protons in the preferred conformation.

Molecular simulations for compounds **2a** and **3a** were performed using the quenched molecular dynamics (QMD) technique,[15,16] that has been used frequently and described in several publications from this laboratory.[17–21] Such simulations generate clusters of low energy conformations without using NMR constraints, hence the technique is not biased in any way toward the conclusions that could be reached from the physical experiments. Throughout, the dielectric constant of the medium for the calculations was set at 45 to simulate DMSO.

Table 3 shows the results of the QMD study for compound **2a**. The lowest energy conformer in the cluster of conformers that constitute 'family 1' (F1) has a structure that compares well to a type III β-turn. However, the fit of the physical data for this conformer was poor. The ROE intensities measured for **2a** did not correlate with the interproton distances in that F1-conformer, and some critical coupling constants did not correlate well with values that were calculated from the lowest energy conformer structure. These observations implied that our original premise about structures **2** having β-turn conformations might be incorrect. Moreover, the Cys N*H* proton should have a low temperature coefficient in β-turn conformers but, in fact, it had the highest of the three amide protons. This data strongly suggests the preferred conformation of **2a** is not a β-turn.

Surveying the other families generated in the quenched molecular dynamics study revealed that the lowest energy conformer in family 2 (F2) had characteristics that fit the physical data much better. Comparison of the observed ROE's and the interproton distances gave a reasonably good correlation, and the observed coupling constants were, on average, much closer to the calculated values for that conformer. The structure of this conformer is shown in Fig. 2a. This structure is consistent with the Asn and Cys N*H* protons being neither exceptionally solvent shielded and/or hydrogen bonded, hence having not particularly low temperature coefficients. The Lys N*H* proton having the low temperature coefficient is oriented away from the molecular core. This Lys N*H* proton also had a lower chemical shift value (δ=7.62 ppm compared to 8.37 ppm in **3a**). The simulated orientation of the Lys N*H* proton precludes solvent shielding and H-bonding within the ring. However, it is suitably positioned to H-bond with the Asn side-chain. Indeed, a survey of the conformers generated in F2 demonstrates that this hypothesis regarding the orientation of the Asn side-chain is reasonable (data not shown).

Table 4 shows the results of a similar type of analysis for compound **3a**. In this case the fit of the ROE data does not fit any of the families perfectly, but probably the best match is for family 1 (Fig. 2b). The lowest energy conformer of family 1, and that of all the other families, does not match any turn type. The temperature coefficients for the amide N*H* protons within the macrocycle are relatively large suggesting they may not be involved in H-bonding. This inference was supported by D/H exchange experiments that showed these same hydrogens exchange so fast on the NMR time scale that the process could not be followed conveniently. These data, and the detection of several families in the QMD studies imply that the molecule samples several conformations without finding one that is markedly preferred over the others.

The molecular simulations described above indicate that compound **2a** has a bias towards a β-turn conformation, but in fact the molecule tends to populate the conformation shown in Fig. 2a. The bias towards a particular conformation was less pronounced for compound **3a** on the basis of the CD, molecular simulations, and NMR data. These observations indicate that it is possible that compound **2a** forms a relatively well-defined secondary structure that facilitates the cyclization, relative to compound **3a**. One final experiment was performed to test this assertion. In parallel molecular simulations, fluorinated, linear precursors of compounds **2a** and **3a** were minimized via a molecular mechanics routine, equilibrated at 298 K, then subjected

Table 3. QMD and NMR data for compound **2a**

QMD data					
		Lowest energy conformers			
Residue	Dihedral angle (°)	Family 1	Family 2	Family 3	Family 4
Asn	Φ	−78.57	−73.38	−69.15	−73.58
	Ψ	−31.22	−45.61	−37.31	−21.24
Lys	Φ	−73.34	−95.92	−142.0	−128.7
	Ψ	−18.44	70.26	58.75	35.89
Cys	Φ	−71.93	−138.7	−85.32	−87.26
	Ψ	128.6	130.8	123.6	125.5
Number in family		51	21	13	4
Lowest energy (Kcal/mol)		−1.7146	−1.1014	−0.7915	−0.0352
Distance (Å)CO_i-NH_{i+3}		2.648	3.667	3.161	2.625
Type of turn		β-III	–	–	–

Comparison of ROE with simulated distances					
	ROE	Distances for lowest energy conformers in the four families (Å)			
Benzylic *H*-Asn N*H*	Weak	2.378	2.464	2.383	2.395
	Weak	2.607	2.498	2.571	2.561
Asn N*H*–Lys N*H*	Medium	2.255	2.403	2.577	2.520
Asn $C_\alpha H$–Lys N*H*	Very Weak	3.486	3.530	3.517	3.443
Lys N*H*-Cys N*H*	Weak	2.499	3.587	2.847	2.507
Lys $C_\alpha H$–Cys N*H*	Medium	3.443	2.348	2.493	2.837

Temperature coefficients (ppb/K)		Coupling constants			
		Residue	$^3J_{obs}$ (Hz)	$^3J_{calc}$ (Hz) F-1	F-2
Asn NH	−2.12	Asn	8.0	6.55	5.88
Cys NH	−7.25	Lys	8.0	5.88	8.51
Lys N*H*	−0.79	Cys	9.0	5.69	8.97

to a molecular dynamics simulation for 600 ps at 298 K. A conformer was downloaded every 1 ps throughout the molecular dynamics runs. Fig. 3 plots the distance between the sulfur nucleophile and the electrophilic F–*C* carbon for each of the 600 conformers in the molecular dynamics run. The data for compound **2a** shows that the conformers generated in the first 200 ps of the experiment have a relatively large nucleophile-to-electrophile distance, mostly in the range 10–14 Å. After 220 ps this distance drops to a range that is mostly between 6–10 Å, and stays in this closer range. Molecule **3a** behaved differently under these same conditions. Nucleophile-to-electrophile distances for this molecule did decrease over the course of the molecular dynamics run, but not so abruptly as for the other compound, and the variation in this parameter was greater even in the late stages of the experiment.

Conclusions

The original premise of this work was that molecules **2** would adopt β-turn conformations, whereas members of the series **3** would not, and that this would kinetically favor cyclization for compounds **2** relative to competing reactions. Surprisingly, the conformational analysis presented here indicates that the β-turn conformation was not preferred for **2a**. It is impossible to deduce from these data if the favored conformer of **2a** that was observed prevailed over the β-turn conformers because of a side-chain effect that is particular to the asparagine residue, or if the backbone of systems **2** is intrinsically biased towards this conformation. This treatment also assumes that **2a** and **3a** are representative of all the compounds **2** and **3**, respectively. However, the molecular simulation at ambient temperature does indicate that cyclization of the linear form is statistically favored for compound **2a** relative to compound **3a**. Experimentally, cyclizations to form compounds **2** were indeed more facile than the corresponding cyclizations to give compounds **3** under similar conditions. This study has shown that macrocyclizations of the type being studied in these laboratories do appear to be facilitated if the product has a bias towards a detectable secondary structure. Similar conclusions have been drawn by others on the basis of solution phase studies.[22] Experiments with compound **2a** also illustrate that macrocycles may be designed to adopt β-turn conformations; however, in reality they may not do so because of energetically more favorable conformations that are hard to predict using simple molecular models.

Experimental

General

All α-amino acids used had the L-configuration. All chemicals were obtained from commercial suppliers and used without further purification. Diisopropylcarbodiimide

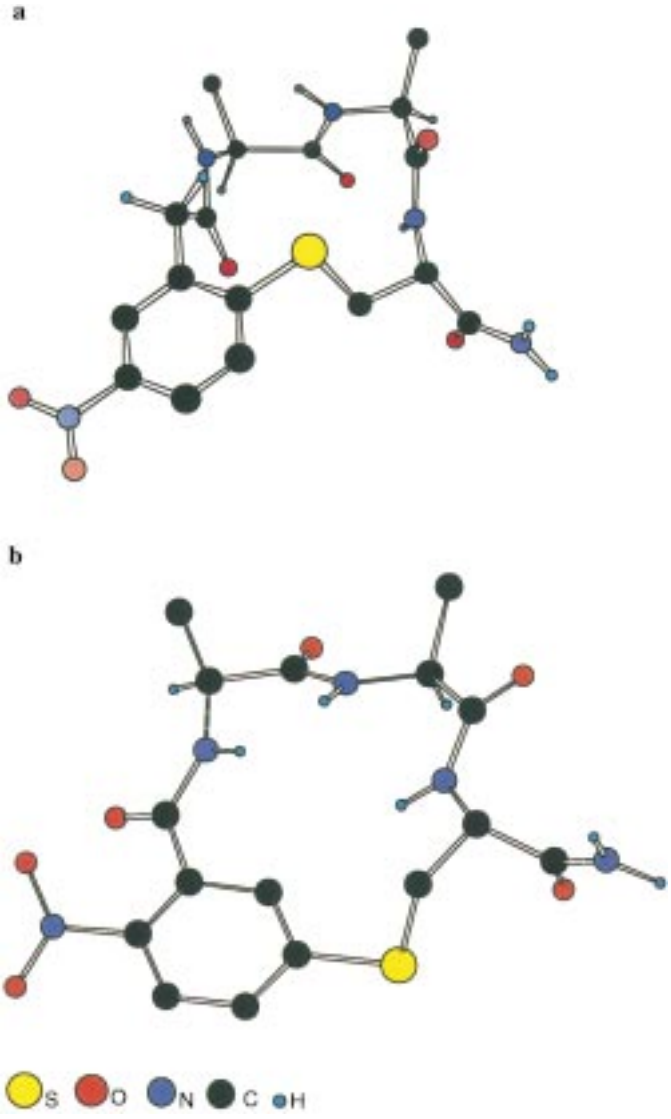

Figure 2. Possible preferred conformations for: **a**, compound **2a**; and, **b**, compound **3a**.

(DIC), *N*-hydroxybenzotriazole (HOBt), trifluoroacetic acid (TFA), oxalyl chloride, piperidine and triisopropylsilane (TIS) were purchased from Aldrich. Dimethylformamide (DMF), methanol, and dichloromethane were bought from EMScience. 5-Fluoro-2-nitrobenzoyl chloride was made by reacting 5-fluoro-2-nitrobenzoic acid (from Fluorochem USA) with oxalyl chloride for 30 min–1 h. 2-Fluoro-5-nitrophenylacetic acid was obtained by nitration of 2-fluorophenylacetic acid (from Aldrich). Rink Amide MBHA resin was purchased from NovaBiochem while TentaGel S Ram Fmoc resin was obtained from Advanced ChemTech. All amino acids used were purchased from either NovaBiochem, Advanced ChemTech or Chem-Impex.

All peptidomimetic syntheses were done in a fritted polypropylene syringe (5 mL capacity) purchased from Torviq. Reverse-phase high-performance liquid chromatography (HPLC) was carried out on Vydac C-18 columns with the following dimensions: 25×0.46 cm for analysis and 25×2.2 cm for preparative work). All HPLC analyses were done using gradient conditions. Eluents used were solvents A (H_2O with 0.1% TFA) and B (CH_3CN with 0.1% TFA). Flow rates applied were 1.0 mL min^{-1} and 6.0 mL min^{-1} for analytical and preparative HPLC respectively.

Solid phase synthesis of peptidomimetics: illustrated for compound 2a

TentaGel S RAM Fmoc (0.05 mmol, 0.26 mmol g^{-1}) was swelled in DMF (ca.10 mL g^{-1}) in a fritted syringe for 1 h. The resin was then washed with DMF (3×at ca. 10 mL g^{-1}, each time for 1 min and all other washings throughout). The Fmoc protecting group on the Rink handle was removed by treating the resin with 20% piperidine in DMF (2×, first for 5 min, then for 25 min). The resin was washed with DMF (3×), MeOH (3×) and CH_2Cl_2 (3×), after which, Fmoc-Cys(Mmt)-OH (3 equiv.), DIC (5 equiv.) and HOBt (5 equiv.) dissolved in DMF (1.5–2 mL) were added. After gentle shaking for about 4–6 h, a ninhydrin test on

Table 4. QMD and NMR data for compound **3a**

QMD data					
		Lowest energy conformers			
Residue	Dihedralangle (°)	Family 1	Family 2	Family 3	Family 4
Asn	Φ	−116.6	66.59	−132.4	−76.34
	Ψ	−41.4	34.39	16.32	−38.91
Lys	Φ	−168.5	−168.9	−172.7	−175.2
	Ψ	45.52	−42.13	−6.409	73.53
Cys	Φ	−80.2	−79.61	−78.02	−78.04
	Ψ	140.0	−30.06	121.7	121.0
Number in family		51	7	40	2
Lowest energy (Kcal/mol)		8.7526	9.2051	8.5837	9.2994
Distance (Å) CO_i–NH_{i+3}		5.224	4.371	4.742	4.532
Type of turn		None fits any turn type			

Comparison of ROE with simulated distances					
	ROE	Distances for lowest energy conformers (Å)			
Aryl *H*–Asn N*H*	Obscured	2.209	1.960	1.925	2.078
Asn N*H*–Lys N*H*	Strong	1.707	2.300	2.027	2.184
Asn $C_\alpha H$–Lys N*H*	Weak	3.518	2.728	3.035	3.515
Lys N*H*–Cys N*H*	Medium	2.261	1.895	1.558	2.786
Lys $C_\alpha H$–Cys N*H*	Strong	2.656	3.530	3.356	2.332

Temperature coefficients (ppb/K)		Coupling constants		
		Residue	$^3J_{obs}$ (Hz)	$^3J_{calc}$(Hz)
Asn N*H*	−2.45	Asn–NH	9.0	9.59
Cys N*H*	−4.49	Lys–NH	9.0	5.65
Lys N*H*	−3.44	Cys–NH	8.5	6.57

sample resin beads gave a negative result. The reaction mixture was then drained and the resin washed with DMF (4×). The above deprotection, coupling and washing cycles were repeated to attach Fmoc-Lys(Boc)-OH, Fmoc-Asn(Trt)-OH and 2-fluoro-5-nitrophenylacetic acid. Removal of the Cys side-chain protecting group (Mmt, 4-methoxytrityl) was carried out using 1% TFA and 5% TIS in CH_2Cl_2 (6×, each time for 10 min). The resin was then washed with CH_2Cl_2 (4×) and was dried for 1 h prior to cyclization. Cyclization was effected by adding K_2CO_3 (5 equiv.) in DMF at 25°C and gently shaking the mixture for ca 24–30 h. The reaction mixture was then drained, the resin was washed with H_2O (5×), DMF (3×), MeOH (3×) and CH_2Cl_2 (3×) and then dried under vacuum for 6 h. The peptide was cleaved from the resin by treatment with a mixture of 90% TFA, 5% TIS and 5% H_2O. The cleavage solution was then separated from the resin by filtration. Most of the cleavage cocktail (ca. 90%) was evaporated in vacuo after which precipitation of the peptide was achieved with anhydrous diethyl ether. The crude peptide was then dissolved in DMF, purified via preparative HPLC (Rainin System, 18–20% B in 20 min) and then lyophilized to give a yellow solid (15 mg, 57%). ^{1}H NMR (500 MHz, DMSO-d_6, 25°C): δ=8.10 (s, 1H), 8.06 (dd, J=2.5, 8.5 Hz, 1H), 7.71 (s, 3H), 7.62 (d, J=8 Hz, 1H), 7.47 (unresolved, 1H), 7.46 (s, 1H), 7.41 (s, 1H), 7.36 (d, J=8 Hz, 1H), 7.28 (bs, 1H), 7.20 (d, J=9 Hz, 1H), 6.94 (s, 1H), 4.62–4.57 (m, 1H), 4.51–4.46 (m,1H), 4.19–4.15 (m, 1H), 3.67–3.10 (m, 2H), 3.65–3.79 (m, 2H), 2.75–2.72 (m, 2H), 2.61–2.47 (m, 2H), 1.69–1.56 (m, 2H), 1.57–1.50 (m, 2H), 1.26–1.21 (m, 2H); ^{13}C NMR (DMSO-d_6, 75 MHz, 25°C): δ=171.3, 171.0, 170.9, 170.7, 168.7, 147.4, 144.1, 134.9, 125.9, 125.7, 122.5, 69.8, 52.8, 52.0, 50.0, 40.4, 38.8, 37.3, 30.0, 26.9, 22.2; analytical HPLC: homogeneous single peak, t_R=9.5 min (8–70% B in 30 min); MALDI MS: calcd for $C_{21}H_{29}N_7O_7S$ $[M\text{H}]^+$ 524.6, found 524.2.

2b. TentaGel S RAM Fmoc resin (0.05 mmol, 0.26 mmol g^{-1}) was used to synthesize this compound. After cleavage from the resin, the crude peptide was purified by preparative HPLC and was lyophilized to give a light yellow solid (13.1 mg, 50%). ^{1}H NMR (DMSO-d_6, 300 MHz, 25°C): δ=8.28–8.23 (m, 2H), 8.107 (d, J=2.4 Hz, 1H), 8.07 (dd, J=2.4 Hz, 1H), 7.70–7.68 (m, 4H), 7.48–7.44 (m, 2H), 7.33 (s, 1H), 4.66–4.58 (m, 1H), 4.25–4.18 (m, 1H), 3.97 (t, J=9 Hz, 1H), 3.83–3.77 (m, 1H), 3.67–3.62 (m, 2H), 3.11 (t, J=11.7 Hz, 1H), 2.76–2.72 (m, 2H), 1.78–1.71 (m, 2H), 1.56–1.49 (m, 4H), 1.29–1.12 (m, 3H), 0.865–0.815 (m, 6H); analytical HPLC: homogeneous single peak, t_R=13.7 min (8–70% B in 30 min); MALDI MS: calcd for $C_{23}H_{34}N_6O_6S$ $[M\text{H}]^+$ 523.6, found 523.2.

2c. TentaGel S RAM Fmoc resin (0.05 mmol, 0.26 mmol g^{-1}) was used to synthesize this compound. After cleavage from the resin, the crude peptide was purified by preparative HPLC and was lyophilized to give a light yellow solid (10.3 mg, 37%). ^{1}H NMR DMSO-d_6, 300 MHz, 25°C): δ=8.29–8.23 (m, 2H), 8.11 (d, J=2.4 Hz, 1H), 8.07 (dd, J=2.4, 2.4 Hz, 1H), 7.72 (d, J=8.1 Hz, 1H), 7.62–7.58 (m, 1H), 7.52 (s, 1H), 7.45 (d, J=8.7 Hz), 7.33 (s, 1H), 4.66–4.58 (m, 1H), 4.27–4.20 (m,

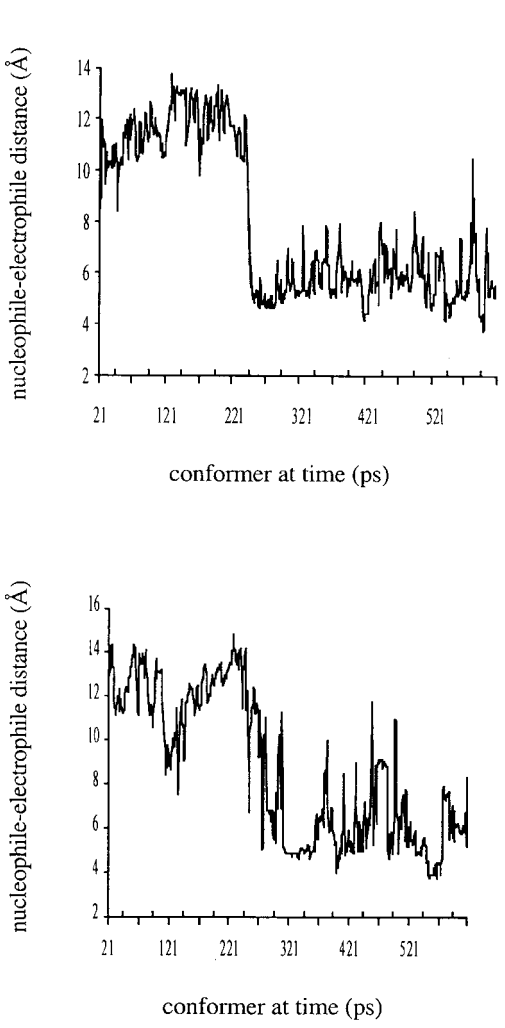

Figure 3. Nucleophile-to-electrophile distances as a function of time in a molecular dynamics simulation (298 K; ϵ=36.7 to mimic DMF) for: **a** compound **2a**; and **b**, compound **3a**.

1H), 4.00–3.94 (m, 1H), 3.82–3.77 (m, 1H) 3.69–3.61 (m, 2H), 3.15–3.07 (m, 3H), 1.76–1.71 (m, 2H), 1.56–1.41 (m, 4H), 1.77–1.13 (m, 1H); analytical HPLC: homogeneous single peak, t_R=15.5 min (8–70 % B in 30 min); MALDI MS: calcd for $C_{23}H_{34}N_8O_6S$ $[M\text{H}]^+$ 551.6, found 551.2.

2d. TentaGel S RAM Fmoc resin (0.05 mmol, 0.26 mmol g^{-1}) was used to synthesize this compound. After cleavage from the resin, the crude peptide was purified by preparative HPLC and was lyophilized to give a yellow solid (9.5 mg, 40 %). ^{1}H NMR (DMSO-d_6, 300 MHz, 25°C):δ=8.68 (d, J=7.8 Hz, 1H), 8.46 (t, J=5.7 Hz, 1H), 8.12 (d, J=2.7 Hz, 1H), 8.04 (dd, J=2.4 Hz, 1H), 7.65–7.62 (m, 2H), 7.45 (d, J=8.1 Hz, 1H) 7.37 (s, 1H), 7.15 (s, 1H), 4.36–4.34 (m, 1H), 4.24–4.21 (m, 1H), 3.88–3.78 (m, 3H), 3.57 (d, J=5.1 Hz, 1H), 3.53–3.35 (m, 6H covered by H_2O signal), 3.13–3.09 (m, 2H), 1.71–1.65 (m, 1H), 1.57–1.42 (m, 3H); analytical HPLC: homogeneous single peak, t_R=10.3 min (8–70% B in 30 min); MALDI MS: calcd for $C_{19}H_{26}N_8O_6S$ $[M\text{H}]^+$ 495.1, found 495.0.

2e. TentaGel S RAM Fmoc resin (0.05 mmol, 0.26 mmol g^{-1}) was used to synthesize this compound. After cleavage from the resin, the crude peptide was purified by preparative HPLC and was lyophilized to give a white solid (15.1 mg, 59%). ^{1}H NMR (DMSO-d_6, 300 MHz, 25°C):δ=8.56–8.54 (m, 1H), 8.11 (d, J=2.4 Hz, 1H), 8.07 (dd, J=6.3 Hz, 1H), 7.86 (d, J=8.7 Hz, 1H) 7.7 (bs, 3H), 7.6 (d, J=8.4 Hz, 1H), 7.5 (d, J=9 Hz, 1H), 7.33 (unresolved, 1H), 7.25 (unresolved, 1H), 4.54–4.51 (m, 1H), 4.25–4.20 (m, 1H), 4.13–4.05 (m, 2H), 3.85–3.71 (m, 2H), 3.60–3.55 (m, 1H), 2.77 (unresolved, 3H), 2.57–2.53 (m, 1H), 1.73–1.70 (m, 2H), 1.59–1.50 (m, 2H), 1.41 (unresolved, 2H), 1.04–1.01 (m, 3H); analytical HPLC: homogeneous single peak, t_R=9.3 min (8–70% B in 30 min); MALDI MS: calcd for $C_{21}H_{30}N_6O_7S$ $[M+\text{Na}]^+$ 533.1, found 533.1.

3a. The same procedure as in that of **2a** was followed except for the following variations. The resin used was Rink Amide MBHA (0.1 mmol, 0.5 mmol g^{-1}). After coupling all amino acids, 5-flouro-2-nitrobenzoyl chloride (4 equiv.) and DIEA (8 equiv.) in CH_2Cl_2 were reacted for 2 h. After cleavage from the resin, the peptide was purified by preparative HPLC (Rainin System, 15–30% B in 30 min) and was lyophilized to give a yellow solid (14.0 mg, 27.5%). ^{1}H NMR (500 MHz, DMSO-d_6, 25°C): δ=8.37 (d, J=9.0 Hz, 1H), 8.01 (d, J=9.0 Hz, 1H), 7.97 (d, J=9.0 Hz, 1H), 7.78 (d, J=8.5 Hz, 1H), 7.70 (bs, 1H), 7.53–7.49 (unresolved, 3H), 7.51 (s, 1H), 7.49 (s, 1H), 7.40 (unresolved, 2H), 7.02 (s, 1H), 4.90–4.87 (m, 1H), 4.44–4.42 (m, 1H), 3.85–3.84 (m, 1H), 3.67–3.42 (m, 2H), 2.77–2.76 (m, 2H), 2.61–2.47 (m, 2H), 1.80–1.77 (m, 1H), 1.54–1.51 (m, 3H), 1.31–1.24 (m, 2H); ^{13}C NMR (DMSO-d_6, 75 MHz, 25°C): δ=171.5, 171.1, 170.8, 170.4, 167.9, 148.5, 140.8, 132.6, 127.7, 124.6, 122.1, 54.5, 52.4, 51.1, 38.6 (overlap with DMSO), 37.2, 22.4, 29.7, 26.7, 21.8 analytical HPLC: homogeneous single peak, t_R=8.3 min (8–70 % B in 30 min); MALDI MS: calcd for $C_{20}H_{27}N_7O_7S$ $[M\text{H}]^+$ 510.5, found 510.1.

3b. Rink amide MBHA (0.05 mmol, 0.54 mmol g^{-1}) was used to synthesize this compound. After cleavage from the resin, the crude peptide was purified by preparative HPLC and was lyophilized to give a yellow solid (4.4 mg, 17.3%). ^{1}H NMR (300 MHz, DMSO-d_6, 25°C): δ=8.07–7.98 (m, 3H), 7.85 (d, J=8.4 Hz, 1H), 7.70 (d, J=8.7 Hz, 1H), 7.62 (s, 3H), 7.28–7.25 (m, 1H) 6.89 (d, J=2.1 Hz, 1H), 6.55 (s, 1H), 4.80–4.77 (m, 1H), 4.52–4.50 (m, 1H), 3.65–3.51 (m, 2H) 3.16–3.11 (m, 1H), 2.74–2.72 (m, 2H), 1.74–1.72 (m, 2H), 1.54–1.48 (m, 4H), 1.26–1.16 (m, 3H), 0.931–0.775 (m, 6H); analytical HPLC: homogeneous single peak, t_R=14.5 min (8–70% B in 30 min); MALDI MS: calcd for $C_{22}H_{32}N_6O_6S$ $[M\text{H}]^+$ 509.6, found 509.2.

3c. Rink amide MBHA (0.05 mmol, 0.54 mmol g^{-1}) was used to synthesize this compound. After cleavage from the resin, the crude peptide was purified by preparative HPLC and was lyophilized to give a yellow solid (5.6 mg, 20.8%). ^{1}H NMR (300 MHz, DMSO-d_6, 25°C): δ= 8.10–7.98 (m, 3H), 7.87 (d, J=8.7 Hz, 1H), 7.63 (s, 1H), 7.55–7.47 (m, 5H) 7.28–7.25 (m, 1H), 6.89 (d, J=2.4 Hz, 2H), 6.55 (s, 1H), 4.79–4.78 (m, 1H), 4.58–4.40 (m, 2H) 4.28–4.18 (m, 1H) 3.61–3.51 (m, 2H), 1.75–1.73 (m, 2H), 1.52–1.48 (m, 4H), 1.22–1.19 (m, 1H), 0.934–0.774 (m, 6H); analytical HPLC: homogeneous single peak, t_R=15.9 min

(8–70% B in 30 min); MALDI MS: calcd for $C_{22}H_{32}N_8O_6S$ $[MH]^+$ 537.6, found 537.2.

3d. Rink amide MBHA (0.05 mmol, 0.54 mmol g^{-1}) was used to synthesize this compound. After cleavage from the resin, the crude peptide was purified by preparative HPLC and was lyophilized to give a yellow solid (5.6 mg, 26.3%). ^{1}H NMR (300 MHz, DMSO-d_6, 25°C): δ=8.15–8.09 (m, 2H), 7.72 (d, J=9.9 Hz, 1H), 7.63 (dd, J=1.8, 2.1 Hz, 1H), 7.45 (s, 1H), 7.30 (s, 1H), 7.23 (d, J=9 Hz, 1H), 7.16 (d, J=2.1 Hz, 1H), 6.53 (s, 1H), 4.91 (bs, 1H), 4.71 (bs, 1H), 4.97 (bs, 1H), 3.79, (d, J=6.3 Hz, 1H), 3.69 (d, J=5.7 Hz, 1H), 3.55–3.50 (m, 2H), 1.16–1.09 (m, 3H); analytical HPLC: homogeneous single peak, t_R=8.1 min (8–70% B in 30 min); MALDI MS: calcd for $C_{16}H_{19}N_5O_7S$ $[MH]^+$ 426.4, found 426.1.

3e. Rink amide MBHA (0.05 mmol, 0.54 mmol g^{-1}) was used to synthesize this compound. After cleavage from the resin, the crude peptide was purified by preparative HPLC and was lyophilized to give a yellow solid (2.5 mg, 10.1%). ^{1}H NMR (300 MHz, DMSO-d_6, 25°C): δ=8.29 (d, J=6.6 Hz, 2H), 8.05 (d, J=9 Hz, 1H), 7.82 (d, J=1H), 7.53 (s, 1H), 7.48 (dd, J=2.4, 2.4 Hz, 1H), 7.45 (s, 1H) 6.98 (d, J=2.1 Hz, 1H), 4.78–4.76 (m, 1H), 4.34 (t, J=9.6 Hz, 1H), 3.64–3.59 (m, 3H), 1.77 (bs, 1H), 1.43 (bs, 2H), 1.04–0.999 (m, 2H), 0.834–0.757 (m, 6H); analytical HPLC: homogeneous single peak, t_R=13.0 min (8–70% B in 30 min); MALDI MS: calcd for $C_{20}H_{25}N_5O_8S$ $[MH]^+$ 496.5, found 496.1.

CD spectra

CD measurements were obtained on an Aviv (model 62 DS) spectrometer. For these experiments the cyclic peptidomimetics were dissolved in H_2O: MeOH (80:20 v/v) (c=0.1 mg mL^{-1}, 0.1 cm path length). The CD spectra were recorded at 25°C.

NMR experiments

NMR spectra were recorded on either a Varian UnityPlus 500 or 300 spectrometer (500 or 300 MHz respectively) for ^{1}H while a 75 MHz was used for ^{13}C. The concentrations of the samples were approximately 5 mM in DMSO-d_6, throughout. One-dimensional (1D) ^{1}H NMR spectra were recorded with a spectral width of 8000 Hz, 32 transients, and a 3 s acquisition time. Vicinal coupling constants were measured from 1D spectra at 25°C. Assignments of ^{1}H NMR resonances in DMSO were performed using sequential connectivities. Temperature coefficients of the amide protons were measured via several 1D experiments in the temperature range 20–50°C adjusted in 5°C increments with an equilibration time of more than 10 min after successive temperature steps.

Two-dimensional (2D) NMR spectra were recorded at 25°C with a spectral width of 8000 Hz. Through-bond connectivities were elucidated by COSY and DQF-COSY spectra, which were recorded with 512 t_1 increments and 16 scans per t_1 increment, with 2 K data points at t_2. Through-space interactions were identified by ROESY spectra. ROESY experiments were performed using mixing times of 100, 200, 300 ms. The intensities of the ROESY cross-peaks were assigned as S (strong), M (medium), and W (weak) from the magnitude of their volume integrals.

Molecular simulations

CHARMm (version 23.2 Revision: 96.0501) was used for the molecular simulations performed in this work. Explicit atom representations were used throughout the study. The residue topology files (RTF) for all the peptidomimetics were built using QUANTA97 (version 97.0711, Molecular Simulations Inc.). Quenched molecular dynamics simulations for **2a** and **3a** were performed using the CHARMm standard parameters. All molecules were modeled in a dielectric continuum of 45 (simulating DMSO). Thus, the starting conformer was minimized using 1000 steps of Steepest Descents (SD) and 3000 steps of the Adopted-Basis Newton Raphson method (ABNR) respectively until an RMS energy derivative of $\leq$0.01 kcal mol^{-1} $Å^{-1}$ was obtained. The minimized structure was then subjected to heating, equilibration, and dynamics simulation. Throughout, the equations of motion were integrated using the Verlet algorithm with a time step 1 fs, and SHAKE was used to constrain all bond lengths containing polar hydrogens. Each peptidomimetic was heated to 1000 K over 10 ps and equilibrated for another 10 ps at 1000 K, then molecular dynamics runs were performed for a total time of 600 ps with trajectories saved every 1 ps. The resulting 600 structures were thoroughly minimized again, using 1000 steps of SD followed by 3000 steps of ABNR. After a suitable cut-off (0.45 and 11.0 kcal mol^{-1} for **2a** and **3a**, respectively), the lowest energy structures were selected for further analysis.

The QUANTA97 package was again used to display and to classify the selected structures into conformational groups. The best clustering was obtained using the grouping method based on calculation of RMS deviation for a subset of atoms, in this study these were the ring backbone atoms. Thus, appropriate threshold values (0.23 and 0.70 Å for **2a** and **3a** respectively) were selected to obtain families with reasonable homogeneity. The lowest energy structure from each family was considered as a favored conformer and thus selected as a representative of the family as a whole. Interproton distances and dihedral angles from the lowest energy structures were calculated for comparisons with the ROE and NMR data.

Molecular dynamics at 25°C was performed starting with linear conformations of compounds **2a** and **3a** were built using QUANTA97, with a (2,4-dimethoxyphenyl)phenyl methine substituent on the *N*-terminus to mimic the structural characteristics of the TentaGel S RAM Fmoc resin. All molecules were modeled in a dielectric continuum of 36.7 (simulating DMF). The starting conformer was minimized using 1000 steps of steepest descents (SD) and 3000 steps of the Adopted-Basis Newton Raphson method until the RMS energy derivative of $\leq$0.01 K cal mol^{-1} $Å^{-1}$ was obtained. Molecular dynamics runs were then performed at 25°C with the minimized conformer. The equation of motions were integrated using the Verlet algorithm with a time step of 1 fs and SHAKE was used to constrain all bond lengths using polar hydrogens. Each

conformer was heated at 298 K over 10 ps, equilibrated at 298 K for another 10 ps, then molecular dynamics simulations were performed, monitoring the distance between the S^- to C(F), for a total time of 600 ps with trajectories saved at every 1 ps. The resulting conformers were then minimized again using 1000 steps of SD followed by 3000 steps of ABNR. After thorough minimization, the monitored distances between the nucleophile and electrophile were tabulated for 600 conformers generated between 21 to 620 ps during the molecular dynamics. The distances were plotted against the conformers generated at every 1 ps to compare the ease of cyclization in both cases.

Acknowledgements

Support for this work was provided by The National Institutes of Health (CA 82642), The Texas Advanced Technology Program, and by The Robert A. Welch Foundation.

References

1. Kahn, M. *Synlett* **1993**, *11*, 821.
2. Feng, Y.; Wang, Z.; Jin, S.; Burgess, K. *J. Am. Chem. Soc.* **1998**, *120*, 10768.
3. Feng, Y.; Wang, Z.; Jin, S.; Burgess, K. *Chemistry—A European J.* **1999**, *5*, 3273.
4. Feng, Y.; Pattarawarapan, M.; Wang, Z.; Burgess, K. *Org. Lett.* **1999**, *1*, 121.
5. Feng, Y.; Burgess, K. *Biotech. Bioeng. Comb. Chem.* **1999**, *71*, 3.
6. Matter, H.; Kessler, H. *J. Am. Chem. Soc.* **1995**, *117*, 3347.
7. Mierke, D. F.; Kessler, H. *J. Am. Chem. Soc.* **1991**, *113*, 9466.
8. Perczel, A.; Hollosi, M.; Turns. In *Circular Dichroism and the Conformational Analysis of Biomolecules*; Fasman, G. D., Ed.; Plenum: New York and London, 1996; p 362.
9. Kopple, K. D.; Ohnishi, M.; Go, A. *J. Am. Chem. Soc.* **1969**, *91*, 4264.
10. Ohnishi, M.; Urry, D. W. *Biochem. Biophys. Res. Commun.* **1969**, *36*, 194.
11. Ohnishi, M.; Urry, D. W. *Biochem. Biophys. Res. Commun.* **1969**, *36*, 194.
12. Dempsey, C. E. *J. Am. Chem. Soc.* **1995**, *117*, 7526.
13. Pardi, A.; Wagner, G.; Wuthrich, K. *Eur. J. Biochem.* **1983**, *137*, 445.
14. Bothner-By, A. A.; Stephen, R. L.; Lee, J.; Warren, C. D.; Jeanloz, R. W. *J. Am. Chem. Soc.* **1984**, *106*, 811.
15. O'Connor, S. D.; Smith, P. E.; Al-Obeidi, F.; Pettitt, B. M. *J. Med. Chem.* **1992**, *35*, 2870.
16. Pettitt, B. M.; Matsunaga, T.; Al-Obeidi, F.; Gehrig, C.; Hruby, V. J.; Karplus, M.; Biophy *J. Biophys. Soc.* **1991**, *60*, 1540.
17. Burgess, K.; Ho, K.-K.; Pettitt, B. M. *J. Am. Chem. Soc.* **1994**, *116*, 799.
18. Burgess, K.; Ho, K.-K.; Pettitt, B. M. *J. Am. Chem. Soc.* **1995**, *117*, 54.
19. Burgess, K.; Ho, K.-K.; Pal, B. *J. Am. Chem. Soc.* **1995**, *117*, 3808.
20. Burgess, K.; Lim, D. *J. Am. Chem. Soc.* **1997**, *119*, 9632.
21. Lim, D.; Moye-Sherman, D.; Ham, I.; Jin, S.; Scholtz, J. M.; Burgess, K. *Chem. Commun.* **1998**, 2375.
22. Adrian, F.; Burguete, M. I.; Luis, S. V.; Miravet, J. F.; Querol, M. *Tetrahedron Lett.* **1999**, *40*, 1039.